ORGANOMETALLICS
Article

Organometallics **2011,** *30,* 717–725 717
DOI: 10.1021/om100840r

Reaction of Spiro[2.4]hepta-4,6-diene with Molybdenum(II) Indenyl Compounds: Effects of Substitution in the Indenyl Ligand

Jan Honzíček,*[,†,‡] Carlos C. Romão,*[,†] Maria J. Calhorda,[§] Abhik Mukhopadhyay,[∥] Jaromír Vinklárek,[‡] and Zdeňka Padělková[‡]

[†]*Instituto de Tecnologia Química e Biológica da Universidade Nova de Lisboa, Av. da República, EAN, 2780-157, Oeiras, Portugal,* [‡]*Department of General and Inorganic Chemistry, Faculty of Chemical Technology, University of Pardubice, Studentská 573, 532 10 Pardubice, Czech Republic,* [§]*Departamento de Química e Bioquímica, CQB, Faculdade de Ciências da Universidade de Lisboa, 1749-016 Lisboa, Portugal, and* [∥]*REQUIMTE/CQFB, Departamento de Química, FCT-UNL, 2829-516 Monte de Caparica, Portugal*

Received August 30, 2010

The series of molybdenum indenyl compounds $[(Ind')Mo(CO)_2(NCMe)_2][BF_4]$ was prepared, and their reactivity toward spiro[2.4]hepta-4,6-diene was studied. It was observed that the spiro-[2.4]hepta-4,6-diene ring opening could be blocked through substitution in the indenyl ring. Hence, the 2-substituted compound $[(\eta^5\text{-}C_9H_6Me)Mo(CO)_2(NCMe)_2][BF_4]$ and 1,3-disubstituted compound $[(\eta^5\text{-}C_9H_5{}^tBu_2)Mo(CO)_2(NCMe)_2][BF_4]$ do not produce the usual *ansa*-compounds but the compounds with η^4-bonded spiro[2.4]hepta-4,6-diene $[(Ind')(\eta^4\text{-}C_5H_4(CH_2)_2)Mo(CO)_2][BF_4]$. The use of 1-substituted compounds $[(\eta^5\text{-}C_9H_6R)Mo(CO)_2(NCMe)_2][BF_4]$ (R = Ph, ^{t}Bu) or compounds with less sterically demanding substituents in the 1,3-positions $[(\eta^5\text{-}C_9H_5Ph_2)Mo(CO)_2(NCMe)_2]$-$[BF_4]$ does not block the ring-opening reaction. These compounds give *ansa*-molybdenocenes $[(Ind')(\eta^5\text{-}C_5H_4CH_2\text{-}\eta^1\text{-}CH_2)Mo(CO)][BF_4]$ in a manner similar to that for the unsubstituted analogue. The reaction products were characterized by NMR and IR spectroscopy. Structures of $[(\eta^5\text{-}C_9H_5Ph_2)Mo(\eta^3\text{-}C_3H_5)(CO)_2]$, $[(\eta^5\text{-}C_9H_6Ph)(\eta^5\text{-}C_5H_4CH_2\text{-}\eta^1\text{-}CH_2)Mo(CO)][BF_4]$, and $[(\eta^5\text{-}C_9H_5Ph_2)(\eta^5\text{-}C_5H_4CH_2\text{-}\eta^1\text{-}CH_2)Mo(CO)][BF_4]$ were determined by single-crystal X-ray analysis.

Introduction

Molybdenocene dichloride (Cp_2MoCl_2) has received great attention, due to its antitumor[1] and catalytic activity.[2] Aqueous solutions of molybdenocene compounds catalyze various processes, including H/D exchange through C−H activation,[3] transfer hydrogenation,[4] nitrile hydration,[5] and hydrolysis of carboxylic acid esters,[5] phosphate esters,[5,6] and thiophosphinates.[7] A part of our research on molybdenocenes[8,9] involves the quest for new ring-substituted compounds with improved biological and catalytic properties.[10]

One of the specific synthetic routes giving molybdenum cyclopentadienyl complexes uses C−C activation of 5,5′-disubstituted cyclopentadienes with molybdenum metal or carbonyls. The transfer of the alkyl group is accompanied by aromatization of the cyclopentadienyl ring and oxidation of the metal center.[11,12] This method was found to be suitable

Scheme 1. Reaction of $[Cp'Mo(CO)_2(NCMe)_2][BF_4]$ (1, Cp′ = Cp; 2, Cp′ = Ind) with Spiro[2.4]hepta-4,6-diene

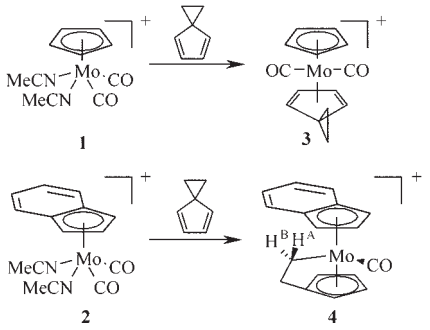

*To whom correspondence should be addressed. E-mail: jan.honzicek@upce.cz (J.H.); ccr@itqb.unl.pt (C.C.R.). Fax: +420/46603 7068 (J.H.); +351-21-441 12 77 (C.C.R.).

(1) (a) Köpf-Maier, P.; Leitner, M.; Voigtlander, R.; Köpf, H. *Z. Naturforsch., C* **1979**, *34*, 1174–1176. (b) Abeysinghe, P. M.; Harding, M. M. *Dalton Trans.* **2007**, 3474–3482. (c) Waern, J. B.; Harding, M. M. *J. Organomet. Chem.* **2004**, *689*, 4655–4668.

(2) Breno, K. L.; Ahmed, T. J.; Pluth, M. D.; Balzarek, C.; Tyler, D. R. *Coord. Chem. Rev.* **2006**, *250*, 1141–1151.

(3) (a) Balzarek, C.; Tyler, D. R. *Angew. Chem., Int. Ed.* **1999**, *38*, 2406–2408. (b) Balzarek, C.; Weakley, T. J. R.; Tyler, D. R. *J. Am. Chem. Soc.* **2000**, *122*, 9427–9434.

(4) Kuo, L. Y.; Finigan, D. M.; Tadros, N. N. *Organometallics* **2003**, *22*, 2422–2425.

(5) Ahmed, T. J.; Zakharov, L. N.; Tyler, D. R. *Organometallics* **2007**, *26*, 5179–5187.

(6) Kuo, L. Y.; Barnes, L. A. *Inorg. Chem.* **1999**, *38*, 814–817.

(7) (a) Kuo, L. Y.; Blum, A. P.; Sabat, M. *Inorg. Chem.* **2005**, *44*, 5537–5541. (b) Kuo, L. Y.; Adint, T. T.; Akagi, A. E.; Zakharov, L. *Organometallics* **2008**, *27*, 2560–2564.

(8) Honzíček, J.; Paz, F. A. A.; Romão, C. C. *Eur. J. Inorg. Chem.* **2007**, 2827–2838.

(9) Honzíček, J.; Mukhopadhyay, A.; Silva, T. S.; Romão, M. J.; Romão, C. C. *Organometallics* **2009**, *28*, 2871–2879.

(10) Ahmed, T. J.; Tyler, D. R. *Organometallics* **2008**, *27*, 2608–2613.

(11) Green, J. C.; Green, M. L. H.; Morley, C. P. *J. Organomet. Chem.* **1982**, *233*, C4–C6.

(12) King, R. B.; Efraty, A. *J. Am. Chem. Soc.* **1971**, *93*, 4950–4952.

Published on Web 02/03/2011

Scheme 2. Synthesis of the Ring-Substituted Indenyl Complexes $[(Ind')Mo(CO)_2(NCMe)_2][BF_4]$ (10−14)

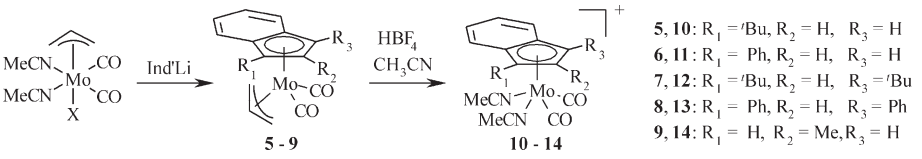

for synthesis of some Cp* ($C_5Me_5^-$) metal complexes when C_5Me_6 or C_5Me_5COOMe is used.[11,13] However, most of the attention has been given to reactions with spirocyclic cyclopentadienes which produce *ansa*-compounds that are suitable precursors for a variety of ring-functionalized compounds.[14,15] In our laboratory, the reactivity of spiro[2.4]hepta-4,6-diene toward the cationic molybdenum complexes $[Cp'Mo(CO)_2(NCMe)_2][BF_4]$ (**1**, Cp′ = Cp; **2**, Cp′ = Ind) was investigated.[8] It was observed that the cyclopentadienyl compound $[CpMo(CO)_2(NCMe)_2][BF_4]$ (**1**) gives the stable η^4-diene complex $[Cp(\eta^4\text{-}C_5H_4(CH_2)_2)Mo(CO)_2][BF_4]$ (**3**), while the indenyl analogue $[IndMo(CO)_2(NCMe)_2][BF_4]$ (**2**) produces the ring-opening product $[Ind(\eta^5\text{-}C_5H_4CH_2\text{-}\eta^1\text{-}CH_2)Mo(CO)][BF_4]$ (**4**) in high yield (see Scheme 1).

A theoretical investigation of these reactions has shown that the discrepancy in the reactivity is a result of activation through $\eta^5-\eta^3$ ring slippage that is favorable in the case of indenyl compounds.[16] However, this haptotropic reactivity enhancement is kinetically controlled and requires a rather subtle, nonobvious series of structural rearrangements of the coordination sphere prior to ring opening. Since such rearrangements are likely to respond to the presence of substituents on the indenyl ring, the present study of the reactivity of spiro[2.4]hepta-4,6-diene with ring-substituted indenyl complexes $[(Ind')Mo(CO)_2(NCMe)_2][BF_4]$ was designed to provide a more detailed insight into the mechanism of the spiro[2.4]hepta-4,6-diene ring-opening reaction.

Results

Synthesis of Ring-Substituted Indenyl Complexes. The cationic indenyl complexes $[(Ind')Mo(CO)_2(NCMe)_2][BF_4]$ (**10**−**14**) were prepared from $[(\eta^3\text{-}C_3H_5)Mo(CO)_2(NCMe)_2X]$ (X = Cl, Br) and the lithium salt of the appropriate indene using the route developed for the unsubstituted analogue **2** (Scheme 2).[17,18]

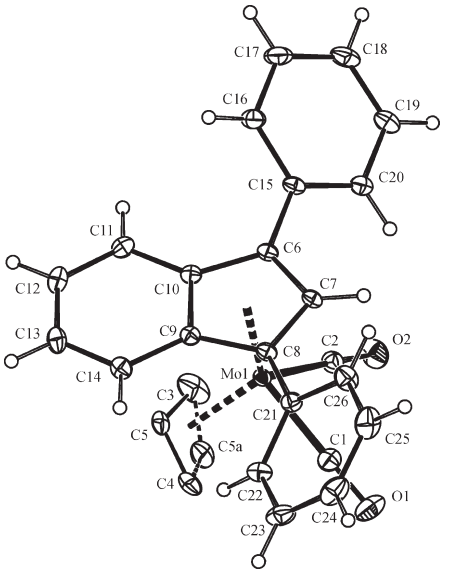

Figure 1. ORTEP drawing of $[(\eta^5\text{-}C_9H_5Ph_2)Mo(\eta^3\text{-}C_3H_5)(CO)_2]$ (**8**). The labeling scheme for all non-hydrogen atoms is shown. Thermal ellipsoids are drawn at the 30% probability level. Hydrogen atoms of the η^3-allyl group have been omitted for clarity. Selected bond lengths (Å) and bond angles (deg): Mo1−C1 = 1.955(3), Mo1−C2 = 1.943(3), Mo1−C6 = 2.373(2), Mo1−C7 = 2.300(2), Mo1−C8 = 2.326(2), Mo1−C9 = 2.414(2), Mo1−C10 = 2.446(2), Mo1−Cg(C6−C10) = 2.0341(10), C1−O1 = 1.155(3), C2−O2 = 1.152(3); C1−Mo1−C2 = 80.57(10), Mo1−C2−O2 = 179.3(2), Mo1−C1−O1 = 178.1(2).

The allyl intermediates $[(Ind')Mo(\eta^3\text{-}C_3H_5)(CO)_2]$ (**5**, **6**, **8**, and **9**) were isolated and characterized by spectroscopic methods. Infrared spectra of these compounds show two bands in the region of CO stretching at ∼1940 and 1860 cm^{-1}. Compounds **5**, **6**, **8**, and **9** form mixtures of *exo* and *endo* isomers in solution, as was evidenced by NMR spectroscopy. At room temperature, the molar ratios between *exo* and *endo* isomers were found to be 4:1 for **5**, 3:1 for **6**, 3.4:1 for **8**, and 3:1 for **9**. The structure of compound **8** was determined by X-ray analysis (Figure 1).

Protonation of $[(Ind')Mo(\eta^3\text{-}C_3H_5)(CO)_2]$ (**5**−**9**) with HBF_4 in the presence of acetonitrile gives the cationic complexes $[(Ind')Mo(CO)_2(NCMe)_2][BF_4]$ (**10**−**14**). NMR measurements prove the coordination of two MeCN ligands and the presence of the η^5-coordinated substituted indenyl ring. The infrared spectra show two bands in the region of terminal carbonyls at ∼1960 (vs) and ∼1870 cm^{-1} (vs) and two bands of the cyano groups at ∼2310 (m) and ∼2280 cm^{-1} (m). The broad band of the B−F stretching at ∼1055 cm^{-1} proves the presence of the BF_4 anion. 1,3-Di-*tert*-butylindene, necessary for the synthesis of **6**, was prepared using the fulvene protocol (see Scheme 3). Condensation of 3-*tert*-butylindene with acetone in the presence of KOH gives 3-*tert*-butyl-1-isopropylideneindene. Subsequent reaction

(13) King, R. B.; Efraty, A. *J. Am. Chem. Soc.* **1972**, *94*, 3773–3779.
(14) (a) Raith, A.; Altmann, P.; Cokoja, M.; Herrmann, W. A.; Kühn, F. E. *Coord. Chem. Rev.* **2010**, *254*, 608–634. (b) Capapé, A.; Raith, A.; Herdtweck, E.; Cokoja, M.; Kühn, F. E. *Adv. Synth. Catal.* **2010**, *352*, 547–556. (c) Capapé, A.; Raith, A.; Kühn, F. E. *Adv. Synth. Catal.* **2009**, *351*, 66–70. (d) Zhao, J.; Jain, K. R.; Herdtweck, E.; Kühn, F. E. *Dalton Trans.* **2007**, 5567–5571. (e) Zhao, J.; Herdtweck, E.; Kuehn, F. E. *J. Organomet. Chem.* **2006**, *691*, 2199–2206. (f) Moriarty, R. M.; Chen, K. M.; Churchill, M. R.; Chang, S. W. Y. *J. Am. Chem. Soc.* **1974**, *96*, 3661–3663. (g) Eilbracht, P. *Chem. Ber* **1976**, *109*, 1429–1435. (h) Eilbracht, P. *Chem. Ber.-Recl.* **1976**, *109*, 3136–3141. (i) Eilbracht, P.; Dahler, P. *J. Organomet. Chem.* **1977**, *127*, C48–C50. (j) Barretta, A.; Chong, K. S.; Cloke, F. G. N.; Feigenbaum, A.; Green, M. L. H. *J. Chem. Soc., Dalton Trans.* **1983**, 861–864. (k) Green, M. L. H.; Ohare, D. *J. Chem. Soc., Dalton Trans.* **1985**, 1585–1590. (l) Chong, K. S.; Green, M. L. H. *Organometallics* **1982**, *1*, 1586–1590.
(15) Amor, F.; Royo, P.; Spaniol, T. P.; Okuda, J. *J. Organomet. Chem.* **2000**, *604*, 126–131.
(16) Veiros, L. F.; Honzíček, J.; Romão, C. C.; Calhorda, M. J. *Inorg. Chim. Acta* **2010**, *363*, 555–561.
(17) Faller, J. W.; Chen, C. C.; Mattina, M. J.; Jakubowski, A. *J. Organomet. Chem.* **1973**, *52*, 361–386.
(18) Ascenso, J. R.; de Azevedo, C. G.; Gonçalves, I. S.; Herdtweck, E.; Moreno, D. S.; Pessanha, M.; Romão, C. C. *Organometallics* **1995**, *14*, 3901–3919.

Scheme 3. Synthesis of 1,3-Di-*tert*-butylindene

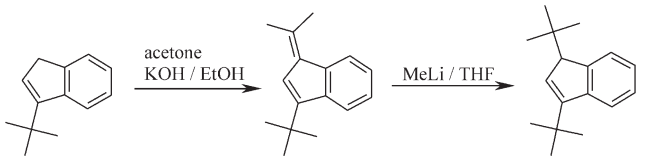

Scheme 4. Reaction of Compounds 10 and 11 with Spiro[2.4]hepta-4,6-diene

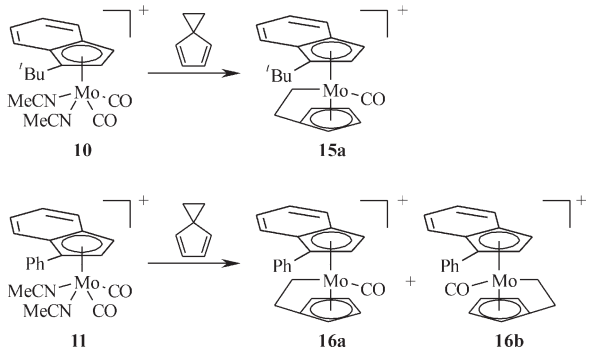

with an excess of MeLi followed by hydrolysis produces the 1,3-di-*tert*-butylindene in 14% overall yield. An alternative pathway giving 1,3-di-*tert*-butylindene uses the reaction of *tert*-butyl chloride with the lithium salt of 3-*tert*-butylindene. Use of this route is limited by very low yields (~ 3%). Other substituted indenes were prepared according to literature procedures.[19−22]

Reaction of [(Ind′)Mo(CO)$_2$(NCMe)$_2$][BF$_4$] (10−14) with Spiro[2.4]hepta-4,6-diene. The replacement of MeCN ligands by spiro[2.4]hepta-4,6-diene leads in most cases to the opening of the cyclopropyl ring and oxidative addition of a C−C bond to the Mo atom, as shown in the examples of Scheme 4. The absence of a plane of symmetry in the 1-substituted indenyl complexes [(Ind′)Mo(CO)$_2$(NCMe)$_2$][BF$_4$] may result in the appearance of two diastereoisomeric products (**a** and **b**) of the ring-opening reaction. However, in practice, a good degree of selectivity is seen in the reaction of spiro-[2.4]hepta-4,6-diene with the *tert*-butylindenyl compound **10** and the phenyl-substituted compound **11**.

Compound **15a** was found to be the sole product of the reaction between **10** and spiro[2.4]hepta-4,6-diene. The phenyl-substituted analogue **11** gives both possible products (**16a**,**b**). The experiments in CD_2Cl_2 followed by NMR spectroscopy have shown that **16a**,**b** appear in the molar ratio 30:1. Multiple recrystallizations from a CH_2Cl_2−hexane mixture give pure isomer **16a**.

The diastereoisomers **a** and **b** were distinguished on the basis of ^{1}H NMR measurements. The methylene proton H^B from the group connected to molybdenum was found to be suitable for this purpose (Scheme 1). Due to the shielding effect of the benzene ring, the indenyl compound [(Ind)(η^5-C$_5$H$_4$CH$_2$-η^1-CH$_2$)Mo(CO)][BF$_4$] (**4**) shows the signal for H^B at much higher field than for its cyclopentadienyl analogue [(Cp)(η^5-C$_5$H$_4$CH$_2$-η^1-CH$_2$)Mo(CO)][BF$_4$] (**3**); see Table 1. A similar effect was observed for isomers **a** and **b**. The compounds **15a** and **16a** show the shift of H^B close to the value observed for the indenyl compound **4**, while the shift in compound **16b** was found to be similar to that of the cyclopentadienyl compound **3**. These differences were assigned to the shielding effect of the benzene. The steric effects cause the monosubstituted compounds to prefer the conformation with the bulky substituent in the position above the OC−Mo−CH$_2$ moiety (see Scheme 4). In this conformation, isomer **a** has the benzene ring of the indenyl on the side of the CH$_2$ group, while isomer **b** has it on the side of the carbonyl ligand. This behavior causes the isomers **a** to exhibit a much stronger effect of the benzene ring than the isomer **b**.

Table 1. Chemical Shifts (ppm) of the CH$_2$Mo Moiety in ^{1}H NMR Spectra of the *ansa*-Compounds [(Cp′)Mo(η^5-C$_5$H$_4$CH$_2$-η^1-CH$_2$)(CO)][BF$_4$]

Cp′	H^A	H^B	ref
η^5-C$_5$H$_5$	−0.41	−0.89	8
η^5-C$_9$H$_7$ (**4**)	−0.07	−3.21	8
η^5-C$_9$H$_6$^{t}Bu (**15a**)	−0.70	−3.05	
η^5-C$_9$H$_6$Ph (**16a**)	−0.09	−3.75	
η^5-C$_9$H$_6$Ph (**16b**)	−0.49	−1.63	
η^5-C$_9$H$_5$Ph$_2$ (**18**)	−0.32	−2.50	

The molecular structure of the compound **16a** obtained from X-ray diffraction analysis (see Figure 2) supports the NMR spectra assignment.

The η^4-diene complex [(η^5-C$_9$H$_5$^{t}Bu$_2$)(η^4-C$_5$H$_4$(CH$_2$)$_2$)-Mo(CO)$_2$][BF$_4$] (**17**) is formed upon reaction of the 1,3-di-*tert*-butyl compound [(η^5-C$_9$H$_5$^{t}Bu$_2$)Mo(CO)$_2$(NCMe)$_2$]-[BF$_4$] (**12**) with spiro[2.4]hepta-4,6-diene (Scheme 5).

The product is stable at room temperature. The reaction of the 1,3-diphenyl analogue **13** gives the *ansa*-compounds [(η^5-C$_9$H$_5$Ph$_2$)(η^5-C$_5$H$_4$CH$_2$-η^1-CH$_2$)Mo(CO)][BF$_4$] (**18**) under the same conditions.

Compounds **17** and **18** were characterized by spectroscopic methods. The ^{1}H NMR spectrum of **17** shows two triplets of the cyclopentadiene protons at 5.54 and 4.19 ppm (^3J(^{1}H,^{1}H) = 2.9 Hz) and two triplets of the methylene groups at 1.36 and 0.67 ppm (^3J(^{1}H,^{1}H) = 8.6 Hz). This pattern is typical for η^4-spiro[2.4]hepta-4,6-diene. The *ansa*-compounds **18** shows four multiplets of the methylene protons at 2.62, 2.34, −0.32, and −2.50 ppm. The signals of the methylene carbons were found at 18.8 and −36.7 ppm. The presence of only one carbonyl group in compound **18** is evident from the infrared spectrum. It shows only one band in the CO stretching region at 2006 cm^{-1}. The molecular structure of compound **18** was determined by X-ray diffraction analysis (see Figure 3).

The compound [(η^5-C$_9$H$_6$Me)Mo(CO)$_2$(NCMe)$_2$][BF$_4$] (**14**) reacts with spiro[2.4]hepta-4,6-diene, giving the η^4-diene complex [(η^5-C$_9$H$_6$Me)(η^4-C$_5$H$_4$(CH$_2$)$_2$)Mo(CO)$_2$][BF$_4$] (**19**) (Scheme 6).

The coordinated spiro[2.4]hepta-4,6-diene gives two triplets of cyclopentadiene at 5.28 and 4.70 ppm (^3J(^{1}H,^{1}H) = 2.9 Hz) and two triplets of the methylene groups at 1.16 and 0.52 ppm (^3J(^{1}H,^{1}H) = 8.4 Hz). These values are similar to those observed for the cyclopentadienyl and 1,3-di-*tert*-butylindenyl analogues [(η^5-C$_5$H$_5$)(η^4-C$_5$H$_4$(CH$_2$)$_2$)Mo(CO)$_2$]-[BF$_4$] (**3**)[8] and [(η^5-C$_9$H$_5$^{t}Bu$_2$)(η^4-C$_5$H$_4$(CH$_2$)$_2$)Mo(CO)$_2$]-[BF$_4$] (**17**), respectively.

(19) Ready, T. E.; Chien, J. C. W.; Rausch, M. D. *J. Organomet. Chem.* **1996**, *519*, 21–28.
(20) Mills, N. S.; Llagostera, K. B.; Tirla, C.; Gordon, S. M.; Carpenetti, D. *J. Org. Chem.* **2006**, *71*, 7940–7946.
(21) Bordwell, F. G.; Drucker, G. E. *J. Org. Chem.* **1980**, *45*, 3325–3328.
(22) Schneider, N.; Huttenloch, M. E.; Stehling, U.; Kirsten, R.; Schaper, F.; Brintzinger, H. H. *Organometallics* **1997**, *16*, 3413–3420.

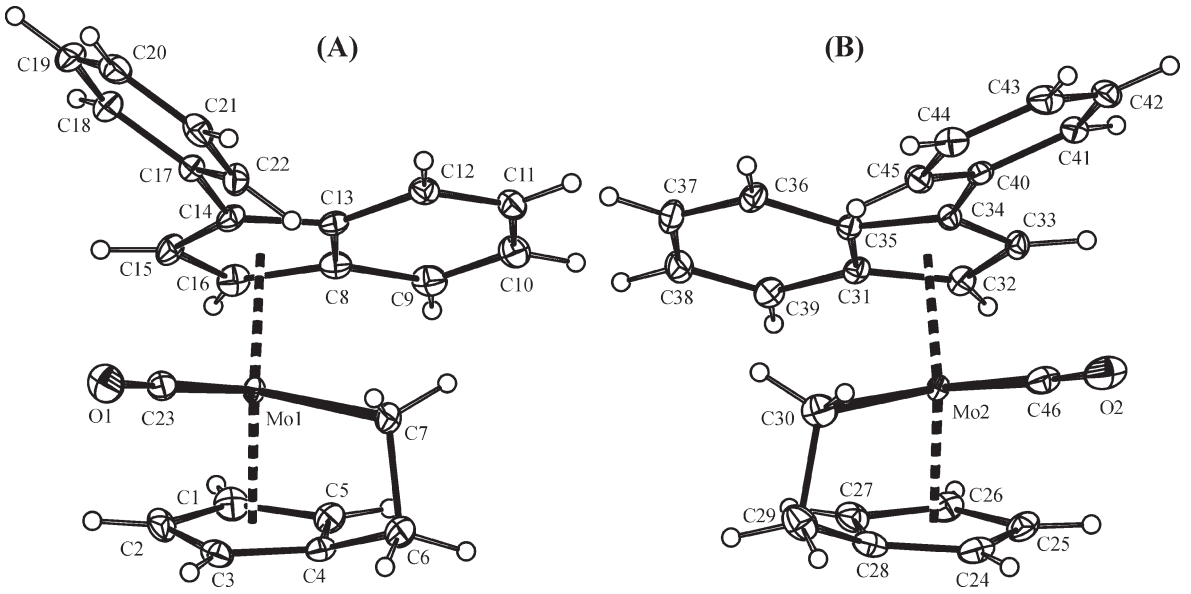

Figure 2. ORTEP drawing of the two crystallographically independent molecules of $[(\eta^5\text{-}C_9H_6Ph)(\eta^5\text{-}C_5H_4CH_2\text{-}\eta^1\text{-}CH_2)Mo(CO)]^+$ present in the crystal structure of **16a** (*S* and *R* configurations). The labeling scheme for all non-hydrogen atoms is shown. Thermal ellipsoids are drawn at the 30% probability level. Selected bond lengths (Å) and bond angles (deg): Mo1−C23 = 1.990(3), Mo1−C7 = 2.280(3), Mo1−Cg(C1−C5) = 1.9501(13), Mo1−Cg(C8−C16) = 2.0152(13), Mo1−C1 = 2.294(3), Mo1−C2 = 2.286(3), Mo1−C3 = 2.290(3), Mo1−C4 = 2.307(3), Mo1−C5 = 2.292(3), Mo1−C8 = 2.369(3), Mo1−C13 = 2.476(3), Mo1−C14 = 2.373(3), Mo1−C15 = 2.288(3), Mo1−C16 = 2.264(3), C23−O1 = 1.138(4), Mo2−C46 = 2.001(3), Mo2−C30 = 2.286(3), Mo2−Cg(C24−C28) = 1.9457(13), Mo2−Cg(C31−C35) = 2.0152(13), Mo2−C24 = 2.287(3), Mo2−C25 = 2.284(3), Mo2−C26 = 2.287(3), Mo2−C27 = 2.289(3), Mo2−C28 = 2.306(3), Mo2−C31 = 2.382(3), Mo2−C32 = 2.276(3), Mo2−C33 = 2.282(3), Mo2−C34 = 2.332(3), Mo2−C35 = 2.464(3), C46−O2 = 1.136(4); C7−Mo1−C23 = 91.29(12), Cg(C1−C5)−Mo1−Cg(C8−C16) = 145.27(6), Mo1−C7−C6 = 101.43(18), Mo1−C23−O1 = 177.3(3), C30−Mo2−C46 = 89.42(13), Cg(C24−C28)−Mo2−Cg(C31−C35) = 144.81(6), Mo2−C28−C29 = 101.49(19), Mo2−C46−O2 = 176.7(3).

Scheme 5. Reaction of 1,3-Disubstituted Compounds 12 and 13 with Spiro[2.4]hepta-4,6-diene

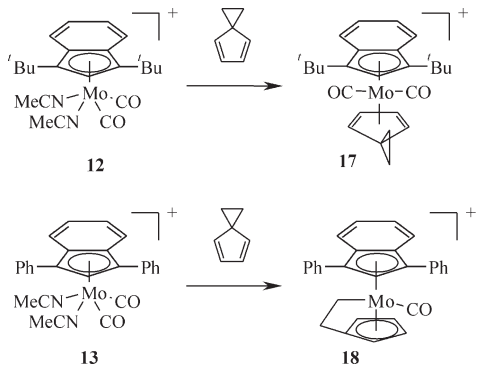

Attempts to observe the intermediates of the reaction between $[(Ind')Mo(CO)_2(NCMe)_2][BF_4]$ (**2**, **10**, **11**, and **13**) and spiro[2.4]hepta-4,6-diene were unsuccessful. The appropriate *ansa*-compounds appear immediately after mixing the starting compounds in CD_2Cl_2 and running the ^1H NMR spectra as fast as possible.

The compounds with coordinated spiro[2.4]hepta-4,6-diene $[(Ind')(\eta^4\text{-}C_5H_4(CH_2)_2)Mo(CO)_2][BF_4]$ (**17** and **19**) are stable at room temperature. All attempts to force the spiro[2.4]hepta-4,6-diene ring-opening reaction by heating or by irradiating their solutions with a tungsten bulb led to decomposition. None of the expected *ansa*-compounds were obtained. Instead, a mixture of intractable products probably due to the polymerization of spiro[2.4]hepta-4,6-diene was formed.

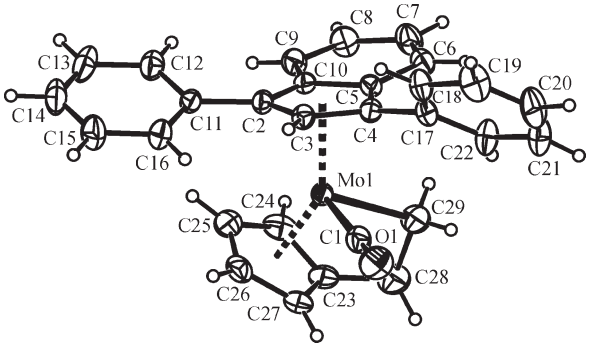

Figure 3. ORTEP drawing of the cation $[(\eta^5\text{-}C_9H_5Ph_2)(\eta^5\text{-}C_5H_4CH_2\text{-}\eta^1\text{-}CH_2)Mo(CO)]^+$ present in the crystal structure of **18**. The labeling scheme for all non-hydrogen atoms is shown. Thermal ellipsoids are drawn at the 30% probability level. Selected bond lengths (Å) and bond angles (deg): Mo1−C1 = 1.999(6), Mo1−C29 = 2.297(6), Mo−Cg(C23−C27) = 1.952(3), Mo−Cg(C2−C10) = 2.009(2), Mo1−C23 = 2.306(6), Mo1−C24 = 2.282(6), Mo1−C25 = 2.290(6), Mo1−C26 = 2.293(6), Mo1−C27 = 2.294(6), Mo1−C2 = 2.305(5), Mo1−C3 = 2.295(5), Mo1−C4 = 2.337(5), Mo1−C5 = 2.439(5), Mo1−C10 = 2.377(5), C1−O1 = 1.126(7); C1−Mo1−C29 = 89.2(3), Cg(C23−C27)−Mo−Cg(C2−C10) = 143.59(12), Mo1−C29−C28 = 101.2(4), Mo1−C1−O1 = 175.2(6).

Crystal Structures. The structure of the allyl complex $[(\eta^5\text{-}C_9H_5Ph_2)Mo(\eta^3\text{-}C_3H_5)(CO)_2]$ (**8**) and the two *ansa*-compounds $[(Ind')(\eta^5\text{-}C_5H_4CH_2\text{-}\eta^1\text{-}CH_2)Mo(CO)][BF_4]$ (**16a**, Ind′ = η^5-C_9H_6Ph; **18**, Ind′ = η^5-$C_9H_5Ph_2$) were determined

Scheme 6. Reaction of Compound 14 with Spiro[2.4]hepta-4,6-diene

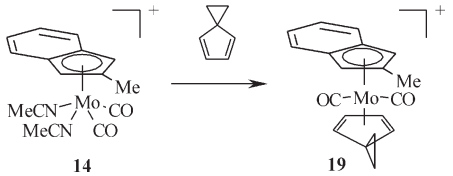

by X-ray diffraction analysis. Their crystallographic data are summarized in Table 2. Compound **16a** has two crystallographically independent complexes in the unit cell that are essentially the same. They are shown in Figure 2.

The molecule of compound **8** has distorted-tetrahedral coordination around Mo(II) with η^3-allyl, η^5-bonded substituted indenyl and two carbonyl ligands (Figure 1). The Mo−C(CO) bond lengths are 1.943(3) and 1.955(3) Å. The C(CO)−Mo−C(CO) bond angle was found to be 80.57(10)°. The distance between the molybdenum atom and the centroid of the η^5-bonded indenyl is 2.0341(10) Å. The Mo−C(Ind) distances vary between 2.300(2) and 2.446(2) Å. The phenyl groups are not coplanar with the indenyl framework. The interplanar angles between phenyl groups and the five-membered ring of the indenyl group are 39.36(12) and 40.16(13)°.

The cations of compounds **16a** and **18** have a bent-metallocene structure with the ligands η^5:η^1-cyclopentadienidoethyl, η^5-bonded substituted indenyl, and one carbonyl. They make a distorted tetrahedron around Mo(IV). The angle Cg(Cp)−Mo−Cg(Ind) was found to be 145.27(6)° for **16a**(**A**), 144.81(6)° for **16a**(**B**), and 143.59(12)° for **18**. The bond angle C(CO)−Mo−C(CH_2) is 91.29(12)° for **16a**(**A**), 89.42(13)° for **16a**(**B**), and 89.2(3)° for **18**. These parameters are similar to those previously obtained for the unsubstituted analogue [(Ind)(η^5-$C_5H_4CH_2$-η^1-CH_2)Mo(CO)][BF_4] (Cg(Ind)−Mo−Cg(Cp) = 145.43(2), 145.43(2)°; C(CO)−Mo−C(CH_2) = 88.5(2), 92.4(2)°).[8] The distance between the molybdenum atom and the centroid of the cyclopentadienyl ligand (1.946(1)−1.952(3) Å) and the bond lengths Mo−C(CH_2) (2.280(3)−2.297(6) Å) are in line with those for other molybdenum(IV) compounds containing an η^5:η^1-cyclopentadienidoethyl ligand (Mo−Cg(Cp) = 1.934−1.983(4) Å, Mo−C(CH_2) = 2.268(5)−2.281(7) Å).[8,23] The bond lengths Mo−C(CO) were found to be 1.990(3) Å for **16a**(**A**), 2.001(3) Å for **16a**(**B**), and 1.999(6) Å for **18**. The distances between molybdenum and the five-membered ring of indenyl are 2.0152(13) Å for **16a**(**A**), 2.0063(12) Å for **16a**(**B**), and 2.009(2) Å for **18**. The phenyl groups are not coplanar with the indenyl framework. The interplanar angles between phenyl groups and the five-membered ring of indenyl vary between 19.4(3) and 44.7(3)°.

Discussion

In light of our previous studies, one would tend to expect that the reactions described here, between the substituted-indenyl complexes [(Ind′)$Mo(CO)_2(NCMe)_2$][BF_4] and spiro[2.4]hepta-4,6-diene, would all end in the corresponding *ansa*-metallocenes as a result of the intramolecular oxidative addition of a C−C bond of the cyclopropyl ring to the Mo(II) ion. Of course, one might expect some rate variations due to the presence of the substituents. In fact, it is usually found that the substitution in the indenyl ring only changes its reactivity slightly, due to the small electronic effects of the substituents.[31] Surprisingly, though, the experimental data presented above show that the reactions of spiro[2.4]hepta-4,6-diene with methyl-, *tert*-butyl-, and phenyl-substituted indenyl molybdenum(II) compounds (**10**−**14**) are quite sensitive to the presence of substituents on the indenyl ring. The mechanism of these ring-opening reactions in the absence of such substituents has been studied in detail by DFT calculations.[16] It was shown that the η^5−η^3 haptotropic rearrangement of the indenyl ligand lowers the barrier of the spiro[2.4]hepta-4,6-diene ring-opening reaction and enables the formation of *ansa*-compounds. However, this haptotropic shift is not a sufficient condition to enable the C−C bond addition to the Mo(II) metal. In fact, the mechanism entails a number of quite subtle structural rearrangements that are responsible for the lowering of the energetic barriers of several of the steps. Part of this mechanism is depicted in Scheme 7, in accord with the DFT calculations already mentioned.[16] Structure **A** is the most stable one for the indenyl spiro-diene complexes. However, opening of the cyclopropyl ring from this structure, even after an $\eta^5 \rightarrow \eta^3$ shift of the indenyl ligand, is hampered by very high activation energies. Several other structures are easily accessible from **A** at room temperature by rotation of the π ligands. Central to this issue is structure **B**, where the OC−Mo−CO group is above the condensed benzene ring of the indenyl ligand and is no longer opposed to it, as in the more stable conformation **A**. DFT calculations show that it is structure **B** that leads to the lower energy pathway toward ring opening. In the first step the $\eta^5 \rightarrow \eta^3$ haptotropic shift of the indenyl opens the coordination sphere of the Mo(II) ion and allows for the oxidative addition of the C−C bond and formation of the new H_2C−Mo bond, leading to intermediate **C**. Upon loss of the CO which is *trans* to the new H_2C−Mo bond the 18e count is restored by the $\eta^3 \rightarrow \eta^5$ indenyl shift. The corresponding structure **D** is only idealized because the whole process following CO loss takes place simultaneously with the structural relaxation toward the metallocene-like structure of the final product **E**. As depicted in Scheme 8, which is a top-down view of intermediate **B**, the cyclopropyl ring must present itself to the Mo atom from a direction either between the indenyl substituents R^1 and R^2 or between the other substituents R^2 and R^3.

Both corresponding conformers **B1** and **B3** are equally accessible and reactive when $R^1 = R^2 = R^3 = H$. However, when bulkier groups are introduced at these positions, differences may arise. When position R^1 is occupied by a bulky group such as ^{t}Bu, conformer **B1** is disfavored and only one product can be formed: that arising from conformer **B3**. Following the expulsion of the CO trans to the new H_2C−Mo bond and the rotation of the new Cp′ ligand (counterclockwise in this case) to form the **E** bent-metallocene-like structure, it is clear that the new Mo−CH_2 bond will be on the same side as R^1. This is exactly what is observed in the formation of **15a** (Scheme 4). In the case where R^1 = Ph, a much less bulky substituent than ^{t}Bu, both conformers **B1** and **B3** can react. However, the product resulting from conformer **B3** will obviously be favored over that resulting from the more hindered **B1**. This is experimentally observed and summarized in Scheme 4 and Figure 2. The product resulting from conformer **B3** (**16a**, with the new H_2C−Mo bond on the same side as the Ph substituent) is

(23) (a) Barretta, A.; Cloke, F. G. N.; Feigenbaum, A.; Green, M. L. H.; Gourdon, A.; Prout, K. *J. Chem. Soc., Chem. Commun.* **1981**, 156–158. (b) Kreiter, C. G.; Wenz, M.; Bell, P. *J. Organomet. Chem.* **1990**, *394*, 195–211.

Table 2. Crystallographic Data of Molybdenum Compounds

	9	16a	18
formula	$C_{26}H_{20}MoO_2$	$C_{23}H_{19}BF_4MoO$	$C_{29}H_{23}BF_4MoO$
formula wt	460.36	494.14	570.22
temp (K)	296(2)	296(2)	150(1)
cryst syst	monoclinic	monoclinic	monoclinic
space group	$P2_1/n$	$P2_1/c$	$P2_1/c$
a (Å)	12.6539(3)	10.6558(4)	9.6430(8)
b (Å)	11.5810(3)	18.9207(8)	11.9781(6)
c (Å)	14.7388(3)	19.6544(8)	22.1769(17)
β (deg)	111.286(1)	92.642 (1)	110.86(1)
V (Å^3)	2012.55(8)	3958.4(3)	2393.6(3)
Z	4	8	4
D_c (g cm^{-3})	1.519	1.658	1.582
μ (mm^{-1})	0.671	0.712	0.600
F(000)	936	1984	1152
cryst size (mm)	0.18 × 0.16 × 0.06	0.30 × 0.18 × 0.04	0.59 × 0.52 × 0.30
θ range (deg)	1.82−30.54	1.49−25.00	1.96−26.6
index ranges	$-18 \le h \le 18$	$-12 \le h \le 10$	$-11 \le h \le 12$
	$-15 \le k \le 16$	$-22 \le k \le 22$	$-14 \le k \le 15$
	$-21 \le l \le 21$	$-23 \le l \le 23$	$-28 \le l \le 27$
no. of rflns collected	36 519	47 438	15 334
no. of indep rflns	5223 (R_{int} = 0.0312)	6096 (R_{int} = 0.0292)	3474 (R_{int} = 0.0714)
no. of params	272	536	325
final R indices ($I > 2\sigma(I)$) [a,b]	R1 = 0.0276	R1 = 0.0264	R1 = 0.0565
	wR2 = 0.0657	wR2 = 0.0659	wR2 = 0.1210
final R indices (all data) [a,b]	R1 = 0.0393	R1 = 0.0305	R1 = 0.0968
	wR2 = 0.0702	wR2 = 0.0754	wR2 = 0.1479
largest diff peak and hole (e Å^{-3})	0.540, −0.712	1.181, −0.481	1.037, −0.922

[a] $R1 = \sum||F_o| - |F_c||/\sum|F_o|$. [b] $wR2 = (\sum[w(F_o^2 - F_c^2)^2]/\sum[w(F_o^2)^2])^{1/2}$.

Scheme 7. Mechanism of the Spiro[2.4]hepta-4,6-diene Ring-Opening Reaction According to Ref 16[a]

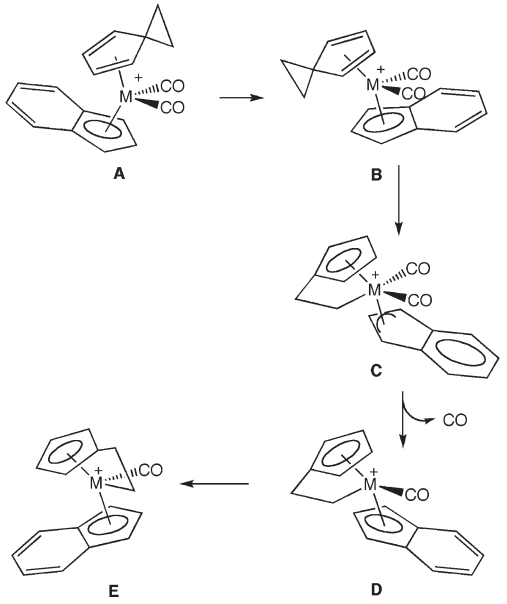

[a] Structure **D** is idealized and is only added to help identify the haptotropic shifts accompanying the reaction. The BF_4^- counterion is omitted.

formed in great excess (30:1) over the product resulting from conformer **B1** (**16b**), which would have the Mo−CO bond over the R^1 = ^{t}Bu substituent. When R^1 = R^3 = ^{t}Bu, both conformers are hindered and the reaction does not proceed because the C_3 ring is in a position unfavorable to approach the Mo ion (see Scheme 5: **17** is stable). Of course, when R^1 = R^3 = Ph the reaction takes place and only one product (**18**) is formed, since there is no energetic difference between **B1** and **B3** (see Scheme 5). We propose that the occupation of the R^2 position in

Scheme 8. Top-Down View of Intermediate B[a]

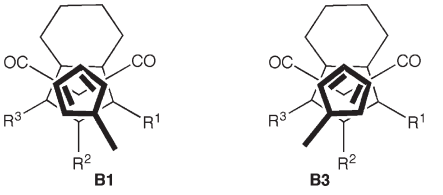

[a] The spiro-diene is on top with the cyclopropyl ring on a plane perpendicular to the paper projecting from the sp^3 carbon. Immediately below the diene plane lies the plane formed by the OC−Mo−CO atoms. The indenyl ring with substituents R^1−R^3 forms the lower, bottom plane. The BF_4^- counterion is omitted.

an intermediate such as **B** hinders the approach of the C_3 ring to the Mo and blocks the reaction. This explains the stability of **19** to ring opening and formation of the corresponding *ansa*-metallocene. This explanation may be corroborated by DFT calculations using indenyl substituted in the R^2 position.

The chemistry just described can be readily explained by the previously published computational predictions on the mechanism of C−C activation of spiro-heptadienes coordinated to $[IndMo(CO)_2]^+$ fragments. Interestingly, the stereoselectivity of the reactions performed with substituents on the indenyl ring was shown to be fully compatible with the structural characteristics of the reaction intermediates that are required by the computational results in order to obtain a reaction pathway with feasible activation energies.

Conclusions

The reaction of several ring-substituted Mo(II) cationic complexes of formula $[(Ind')Mo(CO)_2(NCMe)_2][BF_4]$ with spiro[2.4]hepta-4,6-diene led to a number of different outcomes, depending on the nature and position of those substituents. In the cases where the oxidative addition of the C−C bond of the cyclopropyl ring to the Mo(II) central ion

takes place, the reactions occur within the time of mixing and no intermediates could be detected. When the substituent is in the 1-position (Schemes 4 and 8), two diastereoisomers are produced (**a** and **b**; see Scheme 4) but the formation of the isomer **a** is highly preferred and becomes exclusive when the bulk of the substituent increases to that of ^{t}Bu. When positions 1 and 3 are occupied simultaneously by bulky ^{t}Bu substituents, the oxidative addition of the cyclopropyl ring is sterically hindered and the very stable η^4-diene complex **17** (Scheme 5) is obtained. Similar substitution using Ph instead of ^{t}Bu already allows ready oxidative addition and formation of only one compound (**18**). The presence of one Me group in the 2-position again prevents oxidative addition and leads to the stable η^4-diene complex **19**. This unexpectedly strong reaction discrimination can be easily accommodated by the structural requirements of the C−C oxidative addition reaction that have been previously reported and are elicited by the fluxionality of the cationic $[(\mathrm{Ind}')\mathrm{Mo}(\eta^4\text{-spiro[2.4]hepta-4,6-diene})(\mathrm{CO})_2]^+$.

Experimental Section

Methods and Materials. All operations were performed under nitrogen using conventional Schlenk-line techniques. The solvents were purified and dried by standard methods.[24] Spiro-[2.4]hepta-4,6-diene,[15] 3-*tert*-butylindene,[19] 3-phenylindene,[20] 1,3-diphenylindene,[21] $[(\eta^3\text{-}C_3H_5)Mo(CO)_2(NCMe)_2Cl]$,[17] $[(\eta^3\text{-}C_3H_5)Mo(CO)_2(NCMe)_2Br]$,[25] and $[IndMo(CO)_2(NCMe)_2][BF_4]$ (**2**)[18] were prepared according to literature procedures.

Positive-ion electrospray ionization (ESI) mass spectra were recorded on an API-ION TRAP instrument (PO 03 MS). Samples were measured in CH_2Cl_2 solution. The molybdenum-containing ions had a clearly visible metal isotope pattern, arising from the distribution ^{92}Mo 14.84%, ^{94}Mo 9.25%, ^{95}Mo 15.92%, ^{96}Mo 16.68%, ^{97}Mo 9.55%, ^{98}Mo 24.13%, and ^{100}Mo 9.63%.[26] Spectra obtained were computer-simulated (WSearch32 2005). Mass peaks listed refer to fragments with the isotopes ^{1}H, ^{11}B, ^{12}C, ^{14}N, ^{16}O, ^{19}F, and ^{98}Mo. ^{1}H and ^{13}C{^{1}H} NMR spectra were measured in $CDCl_3$ solutions on a Bruker Avance 400 spectrometer at room temperature. Chemical shifts are given in ppm relative to TMS. IR spectra were recorded in the 4000−440 cm^{-1} region (step 2 cm^{-1}) on a Mattson 7000 FT-IR spectrometer using KBr pellets.

Synthesis of 3-*tert*-Butyl-1-isopropylideneindene. A solution of 3-*tert*-butylindene (8.61 g, 50 mmol) and acetone (8 mL, 110 mmol) in 100 mL of methanol was treated with crushed KOH pellets (5 g, 90 mmol). The mixture was refluxed overnight, giving an orange oil after workup. Vacuum distillation of the crude product gave a yellow oil (bp 120 °C; 100 Pa). Yield: 8.07 g (38 mmol, 76%). ^{1}H NMR ($CDCl_3$; 400 MHz): δ 7.72 (d, $^3J(^1H,^1H)$ = 7.4 Hz, 1H, C_9H_5), 7.56 (d, $^3J(^1H,^1H)$ = 7.5 Hz, 1H, C_9H_5), 7.16 (m, 2H, C_9H_5), 6.52 (s, 1H, C_9H_5), 2.34, 2.21 (2 × s, CH_3), 1.39 (s, 9H, ^{t}Bu). ^{13}C NMR ($CDCl_3$; 101 MHz): δ 150.4, 142.7, 140.1, 137.8, 135.2 ($5C_{ipso}$), 125.5, 124.2, 123.7, 122.0, 121.5 (5C, C_9H_5), 33.2 (C_{ipso}, ^{t}Bu), 29.8 (3C, ^{t}Bu), 24.9, 23.0 (2C, CH_3).

Synthesis of 1,3-Di-*tert*-butylindene. A solution of 3-*tert*-butyl-1-isopropylideneindene (8.07 g, 38 mmol) in THF was treated with methyllithium (60 mmol) and refluxed overnight. The reaction mixture was treated with water and extracted with hexane, giving a yellow oil after workup. Vacuum distillation of the crude product gave a pale yellow oil (bp 100 °C; 100 Pa). Yield: 1.62 g (7 mmol, 18%). ^{1}H NMR ($CDCl_3$; 400 MHz): δ 7.55 (m, 2H, C_9H_6), 7.25 (t, $^3J(^1H,^1H)$ = 7.4 Hz, 1H, C_9H_6), 7.12 (t, $^3J(^1H,^1H)$ = 7.5 Hz, 1H, C_9H_6), 6.19 (s, 1H, C_9H_6), 3.14 (s, 1H, C_9H_6), 1.37 (s, 9H, ^{t}Bu), 1.00 (s, 9H, ^{t}Bu). ^{13}C NMR ($CDCl_3$; 101 MHz): δ 152.7, 148.0, 144.7 ($3C_{ipso}$), 130.3, 125.9, 125.2, 123.7, 122.1 (5C, C_9H_6), 58.8 (1C, C_9H_6), 34.5, 33.2 ($2C_{ipso}$, ^{t}Bu), 29.7, 28.7 (2 × 3C, ^{t}Bu).

Synthesis of $[(\eta^3\text{-}C_3H_5)(\eta^5\text{-}C_9H_6{}^t\mathrm{Bu})Mo(CO)_2]$ (5). 3-*tert*-Butylindene (0.86 g, 5 mmol) was diluted with 30 mL of THF, cooled to 0 °C, and treated dropwise with 3.1 mL of ^{n}BuLi (1.6 mol L^{-1}). The reaction mixture was stirred overnight and then added dropwise to a THF solution of $[(\eta^3\text{-}C_3H_5)Mo(CO)_2(NCMe)_2Cl]$ (1.55 g, 5 mmol) precooled to −80 °C. The reaction mixture was stirred at room temperature overnight and then vacuum-evaporated to dryness. The solid residue was extracted with hexane at 60 °C. The yellow extract was evaporated to dryness in vacuo. The crude product was recrystallized from hexane at −100 °C and dried in vacuo, giving a yellow powder. Yield: 1.42 g (3.9 mmol, 78%). Anal. Calcd for $C_{18}H_{20}MoO_2$: C, 59.34; H, 5.53. Found: C, 59.23; H, 5.75. ^{1}H NMR ($CDCl_3$; 400 MHz; 4:1 mixture of **5a** (*exo*-C_3H_5) and **5b** (*endo*-C_3H_5)): δ 7.60 (m, 1H, C_9H_6), 7.35−7.20 (m, 3H, C_9H_6), 6.13 (d, $^3J(^1H,^1H)$ = 2.8 Hz, 1H of **a**, C_9H_6), 6.03 (d, $^3J(^1H,^1H)$ = 2.9 Hz, 1H of **b**, C_9H_6), 5.81 (d, $^3J(^1H,^1H)$ = 2.8 Hz, 1H of **a**, C_9H_6), 5.77 (d, $^3J(^1H,^1H)$ = 2.9 Hz, 1H of **b**, C_9H_6), 3.73 (dd, $J(^1H,^1H)$ = 6.5 Hz, $J(^1H,^1H)$ = 2.7 Hz, 1H of **b**, *syn* of C_3H_5), 3.65 (dd, $J(^1H,^1H)$ = 6.5 Hz, $J(^1H,^1H)$ = 2.7 Hz, 1H of **b**, *syn* of C_3H_5), 3.54 (m, 1H of **b**, *meso* of C_3H_5), 2.61 (d, $J(^1H,^1H)$ = 7.3 Hz, 1H of **a**, *syn* of C_3H_5), 2.48 (d, $J(^1H,^1H)$ = 7.3 Hz, 1H of **a**, *syn* of C_3H_5), 1.76 (s, 9H, ^{t}Bu), 1.24 (d, $J(^1H,^1H)$ = 11.3 Hz, 1H of **a**, *anti* of C_3H_5), 1.11 (d, $J(^1H,^1H)$ = 11.3 Hz, 1H of **a**, *anti* of C_3H_5), 0.01 (m, 1H of **a**, *meso* of C_3H_5), −0.22 (d, $J(^1H,^1H)$ = 11.0 Hz, 1H of **b**, *anti* of C_3H_5), −0.89 (d, $J(^1H,^1H)$ = 11.0 Hz, 1H of **b**, *anti* of C_3H_5). FTIR (KBr, cm^{-1}): 1940 vs (ν_a(CO)), 1860 vs (ν_s(CO)).

Synthesis of $[(\eta^3\text{-}C_3H_5)(\eta^5\text{-}C_9H_6Ph)Mo(CO)_2]$ (6). The reaction was carried out as was described for compound **5**, but with 3-phenylindene (0.96 g, 5 mmol). The orange oil of the crude product was used for the next reaction without further purification. Yield: 1.52 g (3.9 mmol, 79%). ^{1}H NMR ($CDCl_3$; 400 MHz; 3:1 mixture of **6a** (*exo*-C_3H_5) and **6b** (*endo*-C_3H_5)): δ 7.72−6.95 (m, 5H of C_6H_5 and 4H of C_9H_6), 6.04 (d, $^3J(^1H,^1H)$ = 2.8 Hz, 1H of **a**, C_9H_6), 6.01 (d, $^3J(^1H,^1H)$ = 2.8 Hz, 1H of **a**, C_9H_6), 5.95 (s, 2H of **b**, C_9H_6), 3.50−3.30 (m, 3H of **b**, C_3H_5), 2.34 (d, $J(^1H,^1H)$ = 7.2 Hz, 1H of **a**, *syn* of C_3H_5), 2.07 (d, $J(^1H,^1H)$ = 7.2 Hz, 1H of **a**, *syn* of C_3H_5), 0.94 (d, $J(^1H,^1H)$ = 11.1 Hz, 1H of **a**, *anti* of C_3H_5), 0.84 (d, $J(^1H,^1H)$ = 11.1 Hz, 1H of **a**, *anti* of C_3H_5), 0.68 (m, 1H of **a**, *meso* of C_3H_5), −0.42 (d, $J(^1H,^1H)$ = 10.7 Hz, 1H of **b**, *anti* of C_3H_5), −0.72 (d, $J(^1H,^1H)$ = 10.7 Hz, 1H of **b**, *anti* of C_3H_5). FTIR (KBr, cm^{-1}): 1940 vs (ν_a(CO)), 1856 vs (ν_s(CO)).

Synthesis of $[(\eta^3\text{-}C_3H_5)(\eta^5\text{-}C_9H_5Ph_2)Mo(CO)_2]$ (8). The reaction was carried out as was described for compound **5**, but with 1,3-diphenylindene (1.34 g, 5 mmol). The crude product was recrystallized from hexane and dried in vacuo, giving a yellow powder. Yield: 1.54 g (3.3 mmol, 67%). Anal. Calcd for $C_{26}H_{20}MoO_2$: C, 67.83; H, 4.38. Found: C, 67.94; H, 4.21. ^{1}H NMR ($CDCl_3$; 400 MHz; 3.4:1 mixture of **8a** (*exo*-C_3H_5) and **8b** (*endo*-C_3H_5)): δ 7.78−7.05 (m, 10H of C_6H_5 and 4H of C_9H_5), 6.37 (s, 1H of **a**, C_9H_5), 6.35 (s, 1H of **b**, C_9H_5), 3.40 (d, $J(^1H,^1H)$ = 6.3 Hz, 2H of **b**, *syn* of C_3H_5), 3.33 (m, 1H of **b**, *meso* of C_3H_5), 2.17 (d, $J(^1H,^1H)$ = 7.2 Hz, 2H of **a**, *syn* of C_3H_5), 1.11 (m, 1H of **a**, *meso* of C_3H_5), 0.88 (d, $J(^1H,^1H)$ = 10.9 Hz, 2H of **a**, *anti* of C_3H_5), −0.32 (d, $J(^1H,^1H)$ = 10.7 Hz, 2H of **b**, *anti* of C_3H_5). FTIR (KBr, cm^{-1}): 1946 vs (ν_a(CO)), 1854 vs (ν_s(CO)). Crystals suitable for X-ray analysis were obtained upon cooling of the saturated hexane solution from room temperature to −10 °C.

Synthesis of $[(\eta^3\text{-}C_3H_5)(\eta^5\text{-}C_9H_6Me)Mo(CO)_2]$ (9). The reaction was carried out as was described for compound **5**, but with 2-methylindene (0.65 g, 5 mmol). The crude product was recrystallized from Et_2O/hexane at low temperature and dried in vacuo, giving a yellow powder. Yield: 0.95 g (2.9 g, 59%). Anal. Calcd for $C_{15}H_{14}MoO_2$: C, 55.91; H, 4.38. Found: C, 55.81;

(24) Armarego, W. L. F.; Perrin, D. D. In *Purification of Laboratory Chemicals*; Butterworth-Heinemann: Oxford, U.K., 1996.
(25) Dieck, H. T.; Friedel, H. *J. Organomet. Chem.* **1968**, *14*, 375–385.
(26) Vocke, R. D. *Pure Appl. Chem.* **1999**, *71*, 1593–1607.

H, 4.56. ^{1}H NMR ($CDCl_3$; 400 MHz; 3:1 mixture of **9a** (*exo*-C_3H_5) and **9b** (*endo*-C_3H_5)): δ 7.05−6.85 (m, 4H of C_9H_6), 5.92 (s, 1H of **a**, C_9H_6), 3.43 (d, $J(^1H,^1H)$ = 6.4 Hz, 2H of **b**, *syn* of C_3H_5), 3.27 (m, 1H of **b**, *meso* of C_3H_5), 2.36 (3H, CH_3), 2.27 (d, $J(^1H,^1H)$ = 7.3 Hz, 2H of **a**, *syn* of C_3H_5), 0.88 (d, $J(^1H,^1H)$ = 11.1 Hz, 2H of **a**, *anti* of C_3H_5), 0.19 (m, 1H of **b**, *meso* of C_3H_5), −0.88 (d, $J(^1H,^1H)$ = 11.0 Hz, 2H of **b**, *anti* of C_3H_5). FTIR (KBr, cm^{-1}): 1945 vs (ν_a(CO))], 1858 vs (ν_s(CO)).

Synthesis of [(η^5-$C_9H_6{}^t$Bu)Mo(CO)$_2$(NCMe)$_2$][BF$_4$] (10). [(η^3-C_3H_5)(η^5-$C_9H_6{}^t$Bu)Mo(CO)$_2$] (**5**; 1.30 g, 3.6 mmol) was dissolved in a CH_2Cl_2/MeCN (1/10) mixture, cooled to 0 °C, and treated with 1 equiv of $HBF_4 \cdot Et_2O$. The solution immediately changed color from yellow to dark red. After 10 min the reaction mixture was warmed to room temperature and stirred for an additional 1 h. The reaction mixture was concentrated in vacuo to ∼3 mL, and Et_2O was added to precipitate the red powder. The crude product was recrystallized from CH_2Cl_2/hexane, washed with hexane, and dried in vacuo, giving an orange powder. Yield: 1.60 g (3.3 mmol, 91%). Anal. Calcd for $C_{19}H_{21}BF_4MoN_2O_2$: C, 46.37; H, 4.30; N, 5.69. Found: C, 46.25; H, 4.31; N, 5.88. Positive-ion MS: m/z 366 [M − MeCN]$^+$. Negative-ion MS: m/z 87 [BF$_4$]$^-$. ^{1}H NMR ($CDCl_3$; 400 MHz): δ 7.80 (d, $^3J(^1H,^1H)$ = 8.6 Hz, 1H, C_9H_6), 7.63−7.52 (m, 3H, C_9H_6), 5.87 (d, $^3J(^1H,^1H)$ = 2.6 Hz, 1H, C_9H_6), 4.85(d, $^3J(^1H,^1H)$ = 2.7 Hz, 1H, C_9H_6), 2.42, 2.41 (2 × s, 6H, CH_3CN), 1.42 (s, 9H, ^{t}Bu). ^{13}C NMR ($CDCl_3$; 101 MHz): δ 250.3, 248.6 (2C, *C*O), 139.6, 138.3 (2C, CH_3CN), 131.9, 130.6, 127.6, 126.7 (4C, C_9H_6), 119.0 (2C$_{ipso}$, C_9H_6), 113.0 (C$_{ipso}$, C_9H_6), 87.6, 74.4 (2C, C_9H_6), 33.2 (C$_{ipso}$, ^{t}Bu), 31.5 (3C, ^{t}Bu), 4.4, 4.2 (2C, CH_3CN). FTIR (KBr, cm^{-1}): 2287 m (ν_a(CN)), 2252 m (ν_s(CN)), 1959 vs (ν_a(CO)), 1865 vs (ν_s(CO)), 1055 vs-br (ν_s(BF)).

Synthesis of [(η^5-C_9H_6Ph)Mo(CO)$_2$(NCMe)$_2$][BF$_4$] (11). The reaction was carried out as was described for compound **10**, but with [(η^3-C_3H_5)(η^5-C_9H_6Ph)Mo(CO)$_2$] (**6**; 1.40 g, 3.6 mmol). The crude product was recrystallized from CH_2Cl_2/hexane, washed with hexane, and dried in vacuo, giving an orange powder. Yield: 1.62 g (3.2 mmol, 87%). Anal. Calcd for $C_{21}H_{17}BF_4MoN_2O_2$: C, 49.25; H, 3.35; N, 5.47. Found: C, 49.34; H, 3.58; N, 5.22. Positive-ion MS: m/z 386 [M − MeCN]$^+$. Negative-ion MS: m/z 87 [BF$_4$]$^-$. ^{1}H NMR ($CDCl_3$; 400 MHz): δ 7.87 (d, $^3J(^1H,^1H)$ = 8.4 Hz, 1H, C_9H_6), 7.67−7.37 (m, 3H of C_9H_6 and 5H of C_6H_5), 6.04 (d, $^3J(^1H,^1H)$ = 2.6 Hz, 1H, C_9H_6), 5.37 (d, $^3J(^1H,^1H)$ = 2.7 Hz, 1H, C_9H_6), 2.47, 2.46 (2 × s, 6H, CH_3CN). ^{13}C NMR ($CDCl_3$; 101 MHz): δ 248.1, 247.0 (2C, *C*O), 140.2, 139.4 (2C, CH_3CN), 132.9 (C$_{ipso}$, C_6H_5), 131.9, 131.4 (2C, C_9H_6), 129.4 (2C, C_6H_5), 129.3 (1C, C_6H_5), 128.6 (2C, C_6H_5), 127.1, 125.5 (2C, C_9H_6), 117.7 (2C$_{ipso}$, C_9H_6), 101.5 (C$_{ipso}$, C_9H_6), 88.8, 76.3 (2C, C_9H_6), 4.6, 4.5 (2C, CH_3CN). FTIR (KBr, cm^{-1}): 2310 m (ν_a(CN)), 2279 m (ν_s(CN)), 1962 vs (ν_a(CO)), 1874 vs (ν_s(CO)), 1060 vs-br (ν_s(BF)).

Synthesis of [(η^5-$C_9H_5{}^t$Bu$_2$)Mo(CO)$_2$(NCMe)$_2$][BF$_4$] (12). 1,3-Di-*tert*-butylindene (1.14 g, 5 mmol) was diluted with 30 mL of THF, cooled to 0 °C, and treated dropwise with 3.1 mL of ^{n}BuLi (1.6 mol L^{-1}). The reaction mixture was stirred overnight and then added dropwise to a THF solution of [(η^3-C_3H_5)Mo(CO)$_2$-(NCMe)$_2$Cl] (1.55 g, 5 mmol) precooled to −80 °C. The reaction mixture was stirred at room temperature overnight and then vacuum-evaporated to dryness. The solid residue was extracted with hexane at 60 °C. The yellow extract was evaporated to dryness in vacuo, recrystallized from Et_2O/hexane at −60 °C, and dried in vacuo, giving a yellow powder. The crude [(η^3-C_3H_5)(η^5-C_9H_5-^{t}Bu$_2$)Mo(CO)$_2$] (**7**; 1.5 g, 3.5 mmol) was dissolved in a CH_2Cl_2/MeCN (1/10) mixture, cooled to 0 °C, and treated with 1 equiv of $HBF_4 \cdot Et_2O$. The solution immediately changed color from yellow to dark red. After 10 min the reaction mixture was warmed to room temperature and stirred for an additional 1 h. The reaction mixture was concentrated in vacuo to ∼3 mL, and Et_2O was added to precipitate the red powder. The crude product was recrystallized from CH_2Cl_2/hexane, washed with hexane, and dried in vacuo, giving an orange powder. Yield: 1.47 g (2.7 mmol, 54%). Anal. Calcd for $C_{23}H_{29}BF_4MoN_2O_2$: C, 50.39; H, 5.33; N, 5.11. Found: C, 50.24; H, 5.21; N, 5.39. Positive-ion MS: m/z 422 [M − MeCN]$^+$. Negative-ion MS: m/z 87 [BF$_4$]$^-$. ^{1}H NMR ($CDCl_3$; 400 MHz): δ 7.80 (m, 2H, C_9H_5), 7.58 (m, 2H, C_9H_5), 4.75 (s, 1H, C_9H_5), 2.41 (s, 6H, CH_3CN), 2.41 (s, 18H, ^{t}Bu). ^{13}C NMR ($CDCl_3$; 101 MHz): δ 252.1 (2C, *C*O), 138.8 (2C, CH_3CN), 130.8, 127.7 (2C, C_9H_5), 118.9 (2C$_{ipso}$, C_9H_5), 110.4 (2C$_{ipso}$, C_9H_5), 87.1 (1C, C_9H_5), 33.1 (2C$_{ipso}$, ^{t}Bu), 31.6 (6C, ^{t}Bu), 4.3 (2C, CH_3CN). FTIR (KBr, cm^{-1}): 2315 m [ν_a(CN)], 2289 m [ν_s(CN)], 1960 vs [ν_a(CO)], 1882 vs [ν_s(CO)], 1056 vs-br [ν_s(BF)].

Synthesis of [(η^5-$C_9H_5Ph_2$)Mo(CO)$_2$(NCMe)$_2$][BF$_4$] (13). The reaction was carried out as was described for compound **10**, but with [(η^3-C_3H_5)(η^5-$C_9H_5Ph_2$)Mo(CO)$_2$] (**8**; 1.45 g, 3.1 mmol). The crude product was recrystallized from CH_2Cl_2/hexane, washed with hexane, and dried in vacuo, giving an orange powder. Yield: 1.63 g (2.8 mmol, 88%). Anal. Calcd for $C_{27}H_{21}BF_4MoN_2O_2$: C, 55.13; H, 3.60; N, 4.76. Found: C, 54.96; H, 3.23; N, 4.57. Positive-ion MS: m/z 462 [M − MeCN]$^+$. Negative-ion MS: m/z 87 [BF$_4$]$^-$. ^{1}H NMR ($CDCl_3$; 400 MHz): δ 7.89 (m, 2H, C_9H_5), 7.69 (m, 2H, C_9H_5), 7.63 (d, $J(^1H,^1H)$ = 7.4 Hz, 4H, C_6H_5), 7.52−7.40 (m, 6H, C_6H_5), 5.75 (s, 1H, C_9H_5), 2.51 (s, 6H, CH_3CN). FTIR (KBr, cm^{-1}): 2319 m (ν_a(CN)), 2286 m (ν_s(CN)), 1972 vs (ν_a(CO)), 1903 vs (ν_s(CO)), 1056 vs-br (ν_s(BF)).

Synthesis of [(η^5-C_9H_6Me)Mo(CO)$_2$(NCMe)$_2$][BF$_4$] (14). The reaction was carried out as was described for compound **10**, but with [(η^3-C_3H_5)(η^5-C_9H_6Me)Mo(CO)$_2$] (**9**; 0.80 g, 2.5 mmol). The crude product was recrystallized from CH_2Cl_2/hexane, washed with hexane, and dried in vacuo, giving an orange powder. Yield: 1.02 g (2.3 mmol, 91%). Anal. Calcd for $C_{16}H_{15}BF_4MoN_2O_2$: C, 42.70; H, 3.36; N, 6.22. Found: C, 42.51; H, 3.14; N, 6.01. Positive-ion MS: m/z 324 [M − MeCN]$^+$. Negative-ion MS: m/z 87 [BF$_4$]$^-$. ^{1}H NMR ($CDCl_3$; 400 MHz): δ 7.51 (m, 4H, C_9H_6), 5.90 (s, 2H, C_9H_6), 2.43 (s, 6H, CH_3CN), 1.88 (s, 3H, CH_3). ^{13}C NMR ($CDCl_3$; 101 MHz): δ 249.7 (2C, *C*O), 139.9 (2C, CH_3CN), 131.3 (2C, C_9H_6), 126.2 (2C, C_9H_6), 118.4 (2C$_{ipso}$, C_9H_6), 78.6 (2C, C_9H_6), 110.4 (2C$_{ipso}$, C_9H_5), 108.7 (1C$_{ipso}$, C_9H_6), 15.5 (1C, CH_3), 4.5 (2C, CH_3CN). FTIR (KBr, cm^{-1}): 2293 m (ν_a(CN)), 2253 m (ν_s(CN)), 1948 vs (ν_a(CO)), 1875 vs (ν_s(CO)), 1060 vs-br (ν_s(BF)).

Synthesis of [(η^5-$C_9H_6{}^t$Bu)(η^5-$C_5H_4CH_2$-η^1-CH_2)Mo(CO)]-[BF$_4$] (15). A solution of [(η^5-$C_9H_6{}^t$Bu)Mo(CO)$_2$(NCMe)$_2$][BF$_4$] (**10**; 0.20 g, 0.4 mmol) in CH_2Cl_2 (20 mL) was treated with an excess of spiro[2.4]hepta-4,6-diene (0.1 g, 1.1 mmol). After it was stirred for 15 min, the reaction mixture was concentrated in vacuo to ca. 3 mL. Addition of Et_2O precipitated an orange powder that was recrystallized from CH_2Cl_2/Et_2O. Yield: 0.18 g (0.38 mmol, 93%). Anal. Calcd for $C_{21}H_{23}BF_4MoO$: C, 53.19; H, 4.89. Found: C, 53.36; H, 4.73. Positive-ion MS: m/z 389 [M]$^+$. Negative-ion MS: m/z 87 [BF$_4$]$^-$. ^{1}H NMR ($CDCl_3$; 400 MHz): δ 7.67 (d, $^3J(^1H,^1H)$ = 8.5 Hz, 1H, C_9H_6), 7.50−7.42 (m, 2H, C_9H_6), 7.32 (m, 1H, C_9H_6), 6.50 (m, 1H, C_5H_4), 6.38 (d, $^3J(^1H,^1H)$ = 3.5 Hz, 1H, C_9H_6), 5.63 (d, $^3J(^1H,^1H)$ = 3.5 Hz, 1H, C_9H_6), 5.56, 4.90, 4.73 (3 × m, 3H, C_5H_4), 2.54 (m, 6 lines, 1H, CH_2CH_2Mo), 2.31 (m, 6 lines, 1H, CH_2CH_2-Mo), 1.44 (s, 9H, ^{t}Bu), −0.70 (m, 5 lines, 1H, CH_2CH_2Mo), −3.05 (m, 7 lines, 1H, CH_2CH_2Mo). ^{13}C NMR ($CDCl_3$; 101 MHz): δ 228.5 (1C, *C*O), 131.6, 130.0, 127.5, 124.3 (4C, C_9H_6), 117.2, 112.5, 110.5 (3C$_{ipso}$, C_9H_6), 97.1, 92.7, 90.1 (3C, C_5H_4), 84.9 (1C, C_9H_6), 81.6 (1C, C_5H_4), 81.4 (1C, C_9H_6), 80.6 (C$_{ipso}$, C_5H_4), 33.8 (C$_{ipso}$, ^{t}Bu), 31.5 (3C, ^{t}Bu), 18.6 (1C, CH_2-CH_2Mo), −38.5 (1C, CH_2CH_2Mo). FTIR (KBr, cm^{-1}): 1999 vs (ν(CO)), 1056 vs-br (ν_s(BF)).

Synthesis of [(η^5-C_9H_6Ph)(η^5-$C_5H_4CH_2$-η^1-CH_2)Mo(CO)]-[BF$_4$] (16). The reaction was carried out as was described for compound **15**, but with [(η^5-C_9H_6Ph)Mo(CO)$_2$(NCMe)$_2$][BF$_4$] (**11**; 0.20 g, 0.4 mmol). The product recrystallized from CH_2Cl_2/Et_2O contains a 30:1 mixture of **16a** and **16b**. Repeated recrystallization from a CH_2Cl_2/hexane mixture gives a pure sample of **16a**. Yield: 0.17 g (0.34 mmol, 88%). Anal. Calcd for $C_{23}H_{19}BF_4MoO$: C, 55.90; H, 3.88. Found: C, 55.61; H, 3.72. Positive-ion

MS: m/z 409 $[M]^+$. Negative-ion MS: m/z 87 $[BF_4]^-$. ^1H NMR ($CDCl_3$; 400 MHz) of **16a**: δ 7.93 (d, $^3J(^1H,^1H)$ = 8.8 Hz, 1H, C_9H_6), 7.62 (m, 1H, C_9H_6), 7.56−7.39 (m, 2H of C_9H_6, and 5H of C_6H_5), 6.77 (m, 1H, C_5H_4), 6.65 (d, $^3J(^1H,^1H)$ = 3.5 Hz, 1H, C_9H_6), 6.02 (d, $^3J(^1H,^1H)$ = 3.5 Hz, 1H, C_9H_6), 5.67, 4.73, 4.58 (3 × m, 3H, C_5H_4), 2.46 (m, 6 lines, 1H, CH_2CH_2Mo), 2.36 (m, 6 lines, 1H, CH_2CH_2Mo), −0.09 (m, 5 lines, 1H, CH_2CH_2Mo), −3.75 (m, 7 lines, 1H, CH_2CH_2Mo). ^{13}C NMR ($CDCl_3$; 101 MHz) of **16a**: δ 226.5 (1C, CO), 133.1, 130.7, 130.3, 128.1 (3C of C_9H_6 and 1C of C_6H_5), 131.1 (C_{ipso}, C_6H_5), 129.7, 128.3 (2 × 2C, C_6H_5), 122.5 (1C, C_9H_6), 114.4, 106.4, 105.7 (3C_{ipso}, C_9H_6), 98.1, 95.6, 89.8 (3C, C_5H_4), 83.2 (1C, C_9H_6), 82.7 (1C, C_5H_4), 82.1 (1C, C_9H_6), 81.3 (C_{ipso}, C_5H_4), 18.7 (1C, CH_2CH_2Mo), −36.0 (1C, CH_2CH_2Mo). FTIR (KBr, cm^{-1}): 2002 vs (ν(CO))], 1059 vs-br (ν_s(BF)). ^1H NMR ($CDCl_3$; 400 MHz) of **16b** (selected signals): δ −0.49 (m, 5 lines, 1H, CH_2CH_2Mo), −1.63 (m, 5 lines, 1H, CH_2CH_2Mo). Single crystals of **16a** suitable for X-ray analysis were prepared by slow evaporation of the $CDCl_3$ solution.

Synthesis of $[(\eta^5\text{-}C_9H_5{}^tBu_2)(\eta^4\text{-}C_5H_4(CH_2)_2)Mo(CO)_2][BF_4]$ (17). The reaction was carried out as was described for compound **15**, but with $[(\eta^5\text{-}C_9H_5{}^tBu_2)Mo(CO)_2(NCMe)_2][BF_4]$ (**12**; 0.22 g, 0.4 mmol). Yield: 0.14 g (0.24 mmol, 59%). Anal. Calcd for $C_{26}H_{31}BF_4MoO_2$: C, 55.94; H, 5.60. Found: C, 56.29; H, 5.83. ^1H NMR ($CDCl_3$; 400 MHz): 7.79 (m, 2H, C_9H_5), 7.63 (m, 2H, C_9H_5), 5.54 (t, $J(^1H,^1H)$ = 2.9 Hz, 2H, C_5H_4), 5.20 (s, 1H, C_9H_5), 4.19 (t, $J(^1H,^1H)$ = 2.9 Hz, 2H, C_5H_4), 2.42 (s, 18H, ^{t}Bu), 1.36 (t, $^3J(^1H,^1H)$ = 8.6 Hz, 2H, CH_2), 0.67 (t, $^3J(^1H,^1H)$ = 8.6 Hz, 2H, CH_2).

Synthesis of $[(\eta^5\text{-}C_9H_5Ph_2)(\eta^5\text{-}C_5H_4CH_2\text{-}\eta^1\text{-}CH_2)Mo(CO)][BF_4]$ (18). The reaction was carried out as was described for compound **15**, but with $[(\eta^5\text{-}C_9H_5Ph_2)Mo(CO)_2(NCMe)_2][BF_4]$ (**13**; 0.24 g, 0.4 mmol). Yield: 0.22 g (0.39 mmol, 94%). Anal. Calcd for $C_{29}H_{23}BF_4MoO$: C, 61.08; H, 4.07. Found: C, 60.86; H, 3.92. Positive-ion MS: m/z 485 $[M]^+$. Negative-ion MS: m/z 87 $[BF_4]^-$. ^1H NMR ($CDCl_3$; 400 MHz): δ 8.02 (m, 1H, C_9H_5), 7.71 (m, 1H, C_9H_5), 7.62 (m, 6H, C_9H_5 and C_6H_5), 7.53 (m, 4H, C_6H_5), 7.41 (m, 2H, C_6H_5), 6.39 (s, 1H, C_9H_5), 5.53 (m, 1H, C_5H_4), 4.74 (m, 2H, C_5H_4), 4.40 (m, 1H, C_5H_4), 2.62 (m, 6 lines, 1H, CH_2CH_2Mo), 2.34 (m, 8 lines, 1H, CH_2CH_2Mo), −0.32 (m, 6 lines, 1H, CH_2CH_2Mo), −2.50 (m, 7 lines, 1H, CH_2CH_2Mo). ^{13}C NMR ($CDCl_3$; 101 MHz): δ 225.3 (1C, CO), 131.8, 131.6, 130.4, 130.3 (2C of C_6H_5 and 2C of C_9H_5), 131.4, 130.9 (2C_{ipso}, C_6H_5), 130.2, 129.9, 128.2, 127.8 (4 × 2C, C_6H_5), 124.8, 124.6 (2C, C_9H_5), 110.6, 106.7, 103.6, 102.8 (4C_{ipso}, C_9H_5), 105.4, 97.3, 90.3, 85.9, 84.4 (4C of C_5H_4 and 1C of C_9H_5), 80.0 (C_{ipso}, C_5H_4), 18.8 (1C, CH_2CH_2Mo), −36.7 (1C, CH_2CH_2Mo). FTIR (KBr, cm^{-1}): 2006 vs (ν(CO)), 1054 vs-br (ν_s(BF)). Single crystals suitable for X-ray analysis were prepared by careful overlayering of the CH_2Cl_2 solution with hexane.

Synthesis of $[(\eta^5\text{-}C_9H_6Me)(\eta^4\text{-}C_5H_4(CH_2)_2)Mo(CO)_2][BF_4]$ (19). The reaction was carried out as was described for compound **15**, but with $[(\eta^5\text{-}C_9H_6Me)Mo(CO)_2(NCMe)_2][BF_4]$ (**14**; 0.18 g, 0.4 mmol). Yield: 0.10 g (0.22 mmol, 54%). Anal. Calcd for $C_{19}H_{17}BF_4MoO_2$: C, 49.60; H, 3.72. Found: C, 49.88; H, 4.03. ^1H NMR ($CDCl_3$; 400 MHz): 7.67 (m, 2H, C_9H_6), 7.38 (m, 2H, C_9H_6), 6.20 (s, 2H, C_9H_6), 5.28 (t, $J(^1H,^1H)$ = 2.9 Hz, 2H, C_5H_4), 4.70 (t, $J(^1H,^1H)$ = 2.9 Hz, 2H, C_5H_4), 2.26 (s, 3H, CH_3), 1.16 (t, $^3J(^1H,^1H)$ = 8.4 Hz, 2H, CH_2), 0.52 (t, $^3J(^1H,^1H)$ = 8.4 Hz, 2H, CH_2).

X-ray Structure Determination. The measurements of structures **9** and **16a** were carried out on a Bruker SMART APEX CCD diffractometer using graphite-monochromated Mo Kα radiation (λ = 0.710 73 Å) from an X-ray tube. Details of the crystallographic data and refinement parameters are given in Table 2. Programs used: data collection, Smart (Bruker 2003); data reduction, Saint (Bruker version 6); absorption correction, SADABS version 2.10 (Bruker AXS 2001). Structure solution and refinement was done using SHELXTL (Bruker 2003). The structure was solved by direct methods and refined by full-matrix least-squares methods on F^2. The non-hydrogen atoms were refined anisotropically. There is a disordered carbon atom of the C−H fragment originating from the allyl moiety. This disorder was solved by standard constraint and restraint procedures in the SHELXL97 software.[27] The allyl ligand of compound **8** has positional disorder. It was refined in *exo* and *endo* orientations with 60% and 40% occupancy, respectively. The hydrogen atoms of the η^3-allyl were refined only for the major isomer.

The X-ray data (Table 2) for crystals of **18** were obtained at 150 K using an Oxford Cryostream low-temperature device on a Nonius KappaCCD diffractometer with Mo Kα radiation (λ = 0.710 73 Å) and a graphite monochromator. Data reductions were performed with DENZO-SMN.[28] The absorption was corrected by integration methods.[29] Structures were solved by direct methods (Sir92)[30] and refined by full-matrix least squares based on F^2 (SHELXL97).[27] Hydrogen atoms were mostly localized on a difference Fourier map; however, to ensure uniformity of the treatment of the crystal, all hydrogen atoms were recalculated into idealized positions (riding model) and assigned temperature factors U_{iso}(H) = 1.2[U_{eq}(pivot atom)] or 1.5U_{eq} for the methyl moiety with C−H = 0.96, 0.97, and 0.93 Å for methyl, methylene, and hydrogen atoms in aromatic rings or the allyl moiety, respectively.

Crystallographic data for structural analysis have been deposited with the Cambridge Crystallographic Data Centre. Copies of this information may be obtained free of charge from The Director, CCDC, 12 Union Road, Cambridge CB2 1EY, U.K. (fax, +44-1223-336033; e-mail, deposit@ccdc.cam.ac.uk; web, http://www.ccdc.cam.ac.uk).

Acknowledgment. We are grateful to the Czech Science Foundation (GACR, Czech Republic) and Ministry of Education of the Czech Republic (MSM, Czech Republic) for support through projects GACR/203/09/P100 and MSM 0021627501, respectively. J.H. thanks the FCT for the postdoctoral research grant SFRH/BPD/24889/2005. A.M. thanks the FCT for the postdoctoral research grant SFRH/BPD/30142/2006. We thank Cecilia Bonifácio from the FCT-UNL and Paula Brandão from the Universidade de Aveiro for crystal mounting and data collection. We thank the FCT (Portugal) for the funding of the single-crystal diffractometer. The NMR spectrometers are part of the National NMR Network and were acquired with funds from the FCT and FEDER.

Supporting Information Available: CIF files giving crystallographic data for **9**, **16a**, and **18**. This material is available free of charge via the Internet at http://pubs.acs.org.

(27) Sheldrick, G. M. *SHELXL97*; University of Göttingen, Göttingen, Germany, 1997.
(28) Otwinowski, Z.; Minor, W. *Methods Enzymol.* **1997**, *276*, 307–326.
(29) Coppens, P. In *Crystallographic Computing*; Munksgaard: Copenhagen, 1970; pp 255−270.
(30) Altomare, A.; Cascarano, G.; Giacovazzo, C.; Guagliardi, A. *J. Appl. Crystallogr.* **1993**, *26*, 343–350.
(31) (a) King, R. B.; Bisnette, M. B. *Inorg. Chem.* **1965**, *4*, 475–481. (b) Green, M.; McGrath, T. D.; Thomas, R. L.; Walker, A. P. *J. Organomet. Chem.* **1997**, *532*, 61–70.